4-year summary

Opening of the mitochondrial permeability transition (mPT) pore increases the permeability of the inner membrane, leading to mitochondrial swelling and possibly to cell death. The mPT pore opening is inversely related to the magnitude of the proton electrochemical gradient. The module conferring sensitivity of the pore to this gradient has not been identified. We investigated mPT's voltage-sensing properties elicited by calcimycin or H_2O_2 in human fibroblasts exhibiting partial or complete lack of adenine nucleotide translocase 1 (ANT1) and in C2C12 myotubes with knocked-down ANT1 expression. mPT onset was assessed by measuring *in situ* mitochondrial volume using the 'thinness ratio' and the 'cobalt-calcein' technique. De-energization hastened calcimycin-induced swelling in control and partially-expressing ANT1 fibroblasts, but not in cells lacking ANT1, despite greater losses of mitochondrial membrane potential. Matrix Ca^{2+} levels or ADP-ATP exchange rates did not differ among cell types. ANT1-null fibroblasts were also resistant to H_2O_2-induced mitochondrial swelling. Permeabilized C2C12 myotubes with knocked-down ANT1 exhibited higher calcium uptake capacity and voltage-thresholds of mPT opening. We conclude that ANT1 confers sensitivity of the pore to the electrochemical gradient [1].
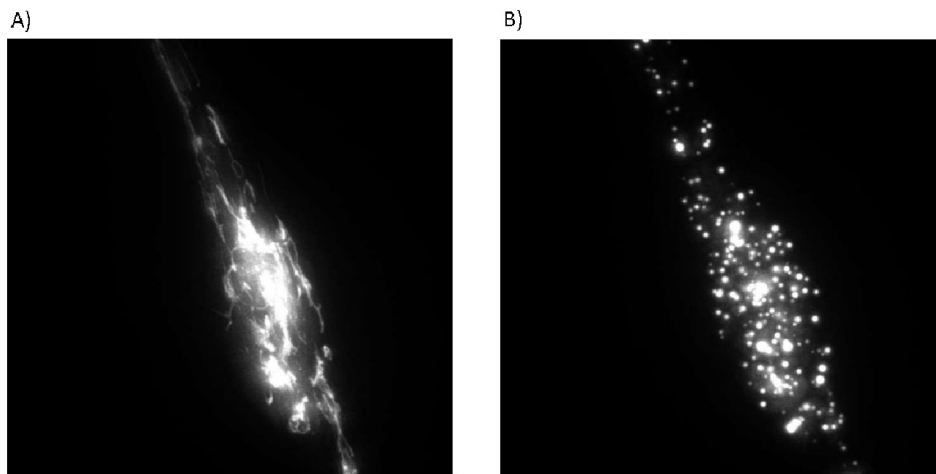

Figure 1. Epifluorescence images of a fibroblast transfected with red fluorescence protein before (A) and after induction of mPT (B).

The mPT pore is involved in aging as well. Cyclophilin D (CypD) is a protein modulating the pore, therefore, we examined the effect of partial or complete cypD deletion on the expression of 18 aging markers, GFAP, mGluR1 and alpha-synuclein in mouse brain. Gender-dependent alterations were detected in the level of these proteins. The life span of the cypD heterozygous but not of the KO mice was increased, but no behavior changes could be observed [2].

Encysted embryos of *Artemia franciscana* have the ability to survive under extreme environmental conditions. The total, mitochondrial and mitoplastic lipid composition of *Artemia franciscana* cysts was identified using high resolution shotgun lipidomics. 1098 lipid species dispersed among 22 different classes were quantitated. *Artemia* mitochondria harboured much less phosphatidylethanolamine, plasmenylethanolamines and ceramides than mitochondria of other species, but exhibited much higher levels of phosphatidylglycerols and phosphatidylserines. The results may contribute to the elucidation of the extremophilia of this species [3].

The *Artemia franciscana* adenine nucleotide translocase (ArANT) was expressed in yeasts and the effect of its heterologous expression on the lipid composition and protein

I

components of the host membrane was investigated. Our results demonstrated that there were both qualitative and quantitative lipidomic changes in the inner mitochondrial membrane of ArANT expressing yeast. Most notably, diacylglycerols, phosphatidylcholines, lysophosphatidylcholines, lysophosphatidylethanolamines, phosphatidylinositols, triacylglycerols and glycolipids were all significantly increased. In addition to the lipidomic changes, the activities of respiratory chain complexes II and IV and of Fo-F1 ATP synthase were decreased, without concomitant alteration in their protein expression levels. The results draw attention to that heterologous expression of membrane proteins can change the lipid environment of the host membrane and thus might alter the function of other membrane-embedded proteins [4].

When oxidative phosphorylation is impaired, mitochondrial substrate-level phosphorylation (SLP) is able to prevent reversal of the ANT and the subsequent mitochondrial consumption of cytosolic ATP. Thus SLP can have a crucial role in the survival of cells under these conditions. We hypothesized that metabolic pathways leading to the accumulation of succinate impair ATP production by this reaction. Mitochondrial SLP was investigated in isolated mouse liver and brain mitochondria using a biosensor test developed by our group. First we verified that GABA, succinic semialdehyde (SSA) and gamma-hydroxybutyrate (GHB) are taken up by mitochondria and metabolized through the GABA shunt. An exception here was GHB which moderately energized liver but not brain mitochondria. Addition of GABA and SSA resulted in impairment of mitochondrial SLP in anoxia, and in the case of GABA this effect was rescued by GABA-transaminase inhibitors. GHB inhibited SLP only in the liver, consistent with the lack of GHB degradation in brain samples. We conclude that the catabolism of these three compounds reduces the ability of mitochondria to perform SLP in anoxia [5].

The NAD^+ required for the operation of SLP under respiratory chain inhibition can be provided by mitochondrial diaphorases, which use different quinone compounds for NADH oxidation. The potential role of a diaphorase enzyme, NAD(P)H:quinone oxidoreductase 1 (Nqo1) in this process was examined. SLP during anoxia or pharmacological inhibition of complex I was compared in liver mitochondria from wild type versus Nqo1$^{-/-}$ mice. The lack of Nqo1 did not affect SLP, implying that the enzyme is dispensable for the operation of the reaction during respiratory inhibition. Based on the idea that quinones potentially support diaphorase function, the effect of different quinone substrates on SLP was compared in the two types of mitochondria. From the examined compounds duroquinone, idebenone and 2-methoxy-1,4-naphtoquinone were able to support SLP when complex I was inhibited, and from these 2-methoxy-1,4-naphtoquinone exerted this beneficial effect as a substrate for Nqo1 [6].

In collaboration with the Rutgers University (Newark, NJ, USA), we analyzed the complete human alpha-ketoglutarate dehydrogenase multienzyme complex (hKGDHc) using hydrogen-deuterium exchange profiles, chemical cross-linking with different cross-linkers, and homology modeling; the analytical method was mass spectrometry. From the analysis of the experimental data we concluded that from the E1 (alpha-ketoglutarate dehydrogenase) component of the complex, the N-terminal region (amino acids 18-40) takes part in the interaction with the other two components, while the thiamine binding region (amino acids 276-330) shows changes when interacting with the E3 (dihydrolipoamide dehydrogenase) component only. In case of E2 (dihydrolipoamide succinyltransferase), we have shown that it interacts with E1 through the lipoyl region and the so called linker region (amino acids 74-132, 194-212). Interestingly, there was no measurable change in hydrogen-deuterium exchange profiles when analyzing the E2 and E3 interaction in the absence of E1. The same conclusion was reached when analyzing the cross-linking data. Component E3 showed low level of interaction with E1, with amino acids 86-146 being the most involved. Based on both

the hydrogen-deuterium and chemical cross-linking data, we started structural modeling of the complex and presently a homology model is being refined. A research article based on these findings was published [7].

The vector constructs of the E1, E2, and the dimerization domain deleted E3 subunits of hKGDHc were prepared for *E. coli* expression. Each protein was purified to homogeneity *via* highly specific FPLC chromatography due to the double Strep-affinity tag which had been added to the N-termini in all the cases and also to the C-terminus of the E1 component sequence. The highly pure enzymes have been being used in structural and functional investigations. E1 subunit was purified *via* a new expression and purification protocol in our collaborative partner laboratory at Rutgers University, as well. The two protein constructs were tested for crystallization at different temperatures. The commercially available screening solutions applied with different concentrations of protein led to promising crystals, which were tested in X-ray diffraction analysis (Helmholtz-Zentrum, Berlin). Nevertheless, further optimization is required in this system. E2 subunit was investigated by cryo-electron microscopy (cryo-EM) in collaboration with the Max Planck Institute of Biochemistry (Munich, Germany) and Central European Institute of Technology (Brno, Czech Republic). The high quality experimental data were processed several times which led to resolution improvement in every step. The final map proved to be of 2.9 Å resolution. The structural model and cryo-EM density map were deposited to the Electron Microscopy Data Bank and Protein Data Bank. E3 subunit lacking the dimerization domain was taken under NMR spectroscopy investigations. Considering the high quantity demand of this technique, proteins were regained from inclusion bodies using refolding. The ^{15}N-labeled subunit was purified from minimum medium expression culture and taken under preliminary NMR analysis at 800 MHz of proton in Gedeon Richter Plc. The initially promising signal dispersion could be further improved by the cleavage of the affinity tag. However, further optimization is required in this system, as well.

Isolipoic acid, a potential ROS generation inhibitor on the E3 subunit was synthesized in collaboration with Bela Noszal's group at Semmelweis University.

The possible synthesis of FAD *via* chemical and enzymatic steps was also studied in detail according to previous literature results. A working synthesis protocol will be essential for future site-specific (isotopic) labeling of this prosthetic group.

Three vector constructs were prepared for the pathogenic mutants of the alpha-ketoadipate dehydrogenase enzyme (E1a) which constitutes the human alpha-ketoadipate dehydrogenase complex together with the E2 and E3 components of hKGDHc. Structural and functional characterization of these disease-causing variants is underway.

We wished to analyze the high-resolution crystal structures of the disease-causing mutants of hE3, the common third subunit of the mitochondrial alpha-keto acid dehydrogenase complexes and also part of the glycine cleavage system. The purpose of this study was to reveal the structural basis of hE3-deficiency with special focus on the mechanism of reactive oxygen species (ROS) production that can be enhanced by certain pathogenic amino acid substitutions. To achieve this goal, a protein crystallography laboratory was set up in 2015 at our department where crystallization of hE3 and nine of its pathogenic mutants has been performed successfully. Data collection was subsequently carried out using synchrotron radiation at BESSY II operated by the Helmholtz-Zentrum Berlin (Berlin, Germany) in collaboration with the Macromolecular Crystallography Group led by Dr. Manfred S. Weiss. As a result, crystal structures were determined for the wild type hE3 with hitherto the highest resolution (1.75 Å) and seven hE3 mutants (D444V-, R447G-, I445M-, R460G-, G426E-, G194C-, and P453L-hE3) in the resolution range of 1.44-2.34 Å. Pathogenic substitutions in the mutants affecting the dimer interface region were found to modulate the properties of a solvent accessible channel leading to the active site. It may be

hypothesized that the triggered changes are capable of impairing H^+/H_2O translocation in the course of the catalytic cycle. An article was published on the comparison of D444V-hE3 and hE3 (see Figure 1) [8]; analysis of the I445M-, R447G-, and R460G-hE3 variants confirmed the theory of a generalized pathomechanism for all the interface mutants (another manuscript on this is going to be submitted for publication shortly). P453L substitution caused major rearrangement of the active site, which can explain the almost complete loss of enzymatic activity of the respective mutant. G194C and G426E substitutions led to minor structural changes, in accord with the least severe clinical symptoms among the mutants.
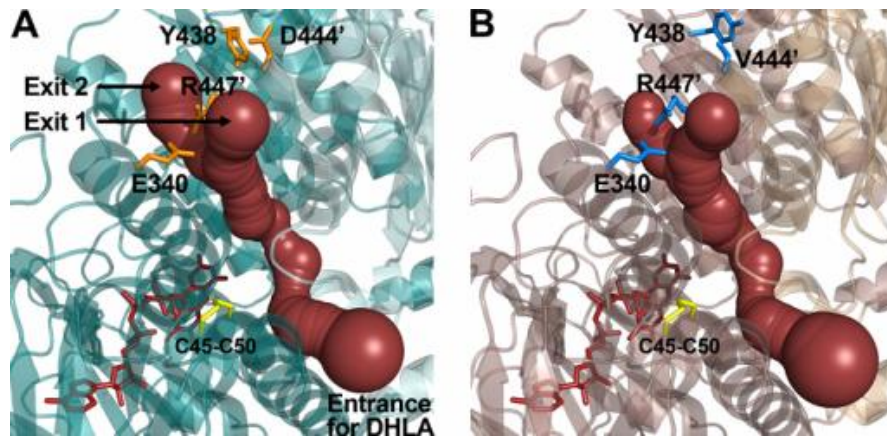

Figure 2. Perturbation of the H^+/H_2O channel in D444V-hE3. Red spheres with the highest possible diameter were placed by the program Caver along the substrate-binding channel and its continuation as H^+/H_2O channel in hE3 (A) and D444V-hE3 (B) to demonstrate channel geometry. D444V substitution led to wider channel cavity after the active site and altered surface polarity near the exit of the channel.

Optimization of crystallization conditions for better diffracting crystals is still an on-going effort for four mutants (E340K-, I358T-, I318T-, and K37E-hE3); I12T, M326V, and G101del substitutions led to highly unstable protein products not making crystallization achievable.

Human dermal fibroblast culture with E3-deficiency from a 4-year-old patient (E340K-hE3, homozygous) arrived from Akron Children's Hospital (Ohio, USA); healthy, normal adult and neonatal fibroblast cultures were also ordered for controls. These cultures have been growing in DMEM for later examinations, like measurements of ATP synthesis rate, reactive oxygen species (ROS) generation rate, membrane potential, oxygen consumption rate (OCR), and extracellular acidification rate (ECAR). Preliminary measurements showed that OCR and growing rate were lower in the mutant cells as compared to the controls; the mutant cells are not capable of growing over 70% confluency.

Bioenergetic experiments on control and KGDHc mutant mouse mitochondria were performed; *DLD* (E3) heterozygotes, *DLST* (E2) heterozygotes, and *DLD/DLST* double knock-out animals were examined. α-ketoglutarate (α-KG)-mediated respiration showed a significant decrease in O_2-consumption in all of the genetically modified animals; the most pronounced decrease was detected in double KO animals. Mitochondria energized with α-KG exhibited a decreased rate of ROS production in all of the KGDH-mutant mice. For DLD heterozygotes we could conclude that *in situ* the E3 subunit plays a major role in ROS production. The decreased rate of H_2O_2 production was also present when mitochondria were energized with non-complex I substrates succinate or alpha-glycerophosphate. The phenomenon of reverse electron transport, i.e. the backflow of electrons from succinate or

alpha-glycerophosphate dehydrogenase to complex I and NAD$^+$, is responsible for the detected decrease in ROS production. E1-3 and gluthatione peroxidase 1 (GPX1) were immunodetected by Western blotting. The expression level of the E1 protein was lower in each type of KGDHc-deficient mice relative to the wild-type. Immunoreactivity of the E2 subunit was decreased in both of the DLST and double KO mice. Surprisingly, the protein level of the E3 subunit was reduced only in the DLD heterozygotes. The GPX 1 immunoreactivity was decreased in the DLST and double KO mice, which was confirmed by enzyme activity measurements, where similar impaired activities were detected in these mitochondria.

In collaboration with Emilia Madarasz's group from MTA-KOKI, we compared the metabolic properties of differentiated neurons and neural stem cells (NSCs). Using the model of *in vitro* neuron production by NE-4C NSCs, this study focused on the metabolic changes taking place during *in vitro* neuronal differentiation. O$_2$-consumption, H$^+$-production, and metabolic responses to single metabolites were measured in cultures of NSCs and in their neuronal derivatives, as well as in primary neuronal and astroglial cultures. In metabolite-free solutions, NSCs consumed little O$_2$ and displayed a higher level of mitochondrial proton leakage than neurons. In stem cells, glycolysis was the main source of energy for the survival of a 2.5-h period of metabolite deprivation. In contrast, stem cell-derived or primary neurons sustained a high-level oxidative phosphorylation during metabolite deprivation, indicating the consumption of their own cellular materials for energy production. The stem cells increased O$_2$-consumption and mitochondrial ATP-production in response to single metabolites (with the exception of glucose), showing rapid adaptation of the metabolic machinery to the available resources. In contrast, single metabolites did not increase the O$_2$-consumption of neurons or astrocytes. In "starving" neurons, neither lactate nor pyruvate was utilized for mitochondrial ATP-production.

A review paper was published on the current knowledge of the various roles of succinate, a well-known metabolite of the citric acid cycle [9]. Succinate besides being an important metabolite at the cross-road of several metabolic pathways, is also involved in the formation and elimination of ROS. However, it is becoming increasingly apparent that its realm extends to epigenetics, tumorigenesis, signal transduction, endo- and paracrine modulation and inflammation. We reviewed the pathways that encompass succinate as a metabolite or signal molecule, and how these may interact under normal and pathological conditions (Figure 3).
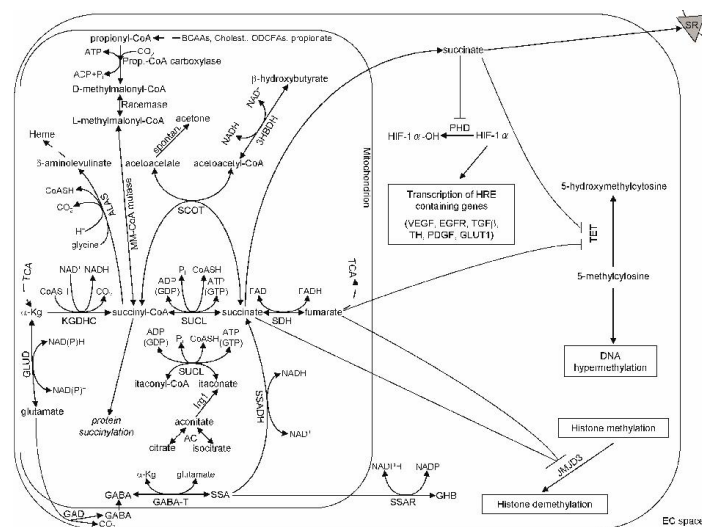
Figure 3. Scheme illustrating the participation of succinate in metabolic and signal transduction pathways. ALAS: δ-aminolevulinate synthase, PHD: prolyl hydroxylases, TET: ten-eleven translocation (TET) family of 5-methylcytosine (5mC) hydroxylases, JMJD3: Jumonji C domain-containing histone lysine demethylases, VEGF: Vascular endothelial growth factor, EGFR: epidermal growth factor receptor, TGFβ: transforming growth factor β, TH: Tyrosine hydroxylase, PDGF: Platelet-derived growth factor, GLUT1 : Glucose transporter 1, BCAAs: Branched-chain amino acids, ODFCAs: odd-number of chain fatty acids, Cholest.: Cholesterol, 3HBDH: 3-hydroxybutyrate dehydrogenase, KGDHC: ketoglutarate dehydrogenase complex, GLUD: glutamate dehydrogenase, GAD: glutamate decarboxylase, GABA: γ-aminobutyric acid, EC space: extracellular space, GABA-T: GABA transaminase, SSA: succinate semialdehyde, SSADH: succinate semialdehyde dehydrogenase, SSAR: succinate semialdehyde reductase, GHB: γ-hydroxybutyric acid, SDH: succinate dehydrogenase; SCOT: Succinyl-CoA:3-Ketoacid Coenzyme A Transferase 1, SR: Succinate Receptor.

Microglia are highly dynamic cells in the brain. Their functional diversity and phenotypic versatility brought microglial energy metabolism into the focus of our research. Although it is known that microenvironmental effects shape microglial phenotype, their bioenergetic response to local nutrient availability remains unclear. Using BV-2 microglial cell line and isolated primary murine microglial cells the effects of various potentially energy donor substrates were investigated in starving microglial cells. Cellular oxygen consumption, glycolytic activity, the levels of intracellular ATP/ADP, autophagy, mTOR phosphorylation, apoptosis, and cell viability were measured in the absence of nutrients or in the presence of physiological energy substrates: glutamine, glucose, lactate, pyruvate, or ketone bodies. Among the metabolic substrates glutamine was able to increase the ATP/ADP ratio and decrease autophagy. All of the respiratory substrates increased both the basal and the maximal respiration. Glucose in microglial cells stimulated the glycolysis, but decreased the oxygen consumption. The ketone body oxidation was significantly stimulated by glutamine. Our data demonstrate the direct metabolic response to nutrients under short-term starvation and that microglia possess versatile metabolic machinery.

Methylene blue (MB), a potential neuroprotective agent, is efficient in various neurodegenerative disease models. The beneficial effects of MB have been attributed to improvements in mitochondrial functions. SLP results in an ATP synthase-independent ATP production. In energetically compromised mitochondria, ATP produced by SLP could prevent the reversal of the adenine nucleotide translocase (ANT) and thus the hydrolysis of glycolytic ATP. ATP that was formed *via* SLP alleviated the energetic insufficiency generated by the lack of oxidative phosphorylation. Thus, the MB-mediated stimulation of SLP might be important in maintaining the energetic competence of mitochondria and in preventing the mitochondrial hydrolysis of glycolytic ATP [10,11].

References:
1. Doczi J, Torocsik B, Echaniz-Laguna A, Mousson de Camaret B, Starkov A, Starkova N, Gál A, Molnár MJ, Kawamata H, Manfredi G, Adam-Vizi V, Chinopoulos C: *Alterations in voltage-sensing of the mitochondrial permeability transition pore in ANT1-deficient cells,* Sci Rep 6:26700, 2016

2. Vereczki V, Mansour J, Pour-Ghaz I, Bodnar I, Pinter O, Zelena D, Oszwald E, Adam-Vizi V, Chinopoulos C: *Cyclophilin D regulates lifespan and protein expression of aging markers in the brain of mice,* Mitochondrion 34:115-126, 2017

3. Chen E, Kiebish MA, McDaniel J, Gao F, Narain NR, Sarangarajan R, Kacso G, Ravasz D, Seyfried TN, Adam-Vizi V, Chinopoulos C: *The total and mitochondrial lipidome of Artemia franciscana encysted embryos,* Biochim Biophys Acta 1861:1727-1735, 2016

4. Chen E, Kiebish MA, McDaniel J, Niedzwiecka K, Kucharczyk R, Ravasz D, Gao F, Narain NR, Sarangarajan R, Seyfried TN, Adam-Vizi V, Chinopoulos C: *Perturbation of the yeast mitochondrial lipidome and associated membrane proteins following heterologous expression of Artemia-ANT,* Sci Rep 8:5915, 2018

5. Ravasz D, Kacso G, Fodor V, Horvath K, Adam-Vizi V, Chinopoulos C: *Catabolism of GABA, succinic semialdehyde or gamma-hydroxybutyrate through the GABA shunt impair mitochondrial substrate-level phosphorylation,* Neurochem Int 109:41-53, 2017

6. Ravasz D, Kacso G, Fodor V, Horvath K, Adam-Vizi V, Chinopoulos C: *Reduction of 2-methoxy-1,4-naphtoquinone by mitochondrially-localized Nqo1 yielding NAD+ supports substrate-level phosphorylation during respiratory inhibition*, Biochim Biophys Acta Bioenerg 1859:909-924, 2018

7. Zhou J, Yang L, Ozohanics O, Zhang X, Wang J, Ambrus A, Arjunan P, Brukh R, Nemeria NS, Furey W, Jordan F: *A multipronged approach unravels unprecedented protein–protein interactions in the human 2-oxoglutarate dehydrogenase multienzyme complex.* J Biol Chem 293:19213-19227, 2018

8. Szabo E, Mizsei R, Wilk P, Zambo Z, Torocsik B, Weiss MS, Adam-Vizi V, Ambrus A: *Crystal structures of the disease-causing D444V mutant and the relevant wild type human dihydrolipoamide dehydrogenase*, Free Radic Biol Med 124: 214-220, 2018

9. Tretter L, Patocs A, Chinopoulos C: *Succinate, an intermediate in metabolism, signal transduction, ROS, hypoxia, and tumorigenesis*, Biochim Biophys Acta 1857:1086-1101, 2016

10. Komlódi T, Tretter L: *Methylene blue stimulates substrate-level phosphorylation catalysed by succinyl-CoA ligase in the citric acid cycle*, Neuropharmacology 123:287-298, 2017

11. Tretter L, Horvath G, Hölgyesi A, Essek F, Adam-Vizi V: *Enhanced hydrogen peroxide generation accompanies the beneficial bioenergetic effects of methylene blue in isolated brain mitochondria,* Free Radic Biol Med 77:317-30, 2014